

A HIGH PERFORMANCE FULLY DIFFERENTIAL PURE CURRENT MODE OPERATIONAL AMPLIFIER AND ITS APPLICATIONS

LEILA SAFARI, SEYED JAVAD AZHARI*

Electrical Engineering Faculty, Iran University of
Science and Technology, Narmak, Tehran Iran

*Corresponding Author: azhari@iust.ac.ir

Abstract

In this paper a novel high performance all current-mode fully-differential (FD) Current mode Operational Amplifier (COA) in BIPOLAR technology is presented. The unique true current mode simple structure grants the proposed COA the largest yet reported unity gain frequency while providing low voltage low power operation. Benefiting from some novel ideas, it also exhibits high gain, high common mode rejection ratio (CMRR), high power supply rejection ratio (PSRR), high output impedance, low input impedance and most importantly high current drive capability. Its most important parameters are derived and its performance is proved by PSPICE simulations using 0.8 μm BICMOS process parameters at supply voltage of $\pm 1.2\text{V}$ indicating the values of 82.4 dB, 52.3°, 31.5 Ω , 31.78 M Ω , 179.2 dB, 2 mW and 698 MHz for gain, phase margin, input impedance, output impedance, CMRR, power and unity gain frequency respectively. Its CMRR also shows very high frequency of 2.64 GHz at zero dB. Its very high PSRR+/PSRR- of 182 dB/196 dB makes the proposed COA a highly suitable block in Mixed-Mode (SOC) chips. Most favourably it can deliver up to ± 1.5 mA yielding a high current drive capability exceeding 25. To demonstrate the performance of the proposed COA, it is used to realize a constant bandwidth voltage amplifier and a high performance Rm amplifier.

Keywords: Fully differential current operational amplifier, Wide band COA, High CMRR COA, Constant bandwidth voltage amplifier, Rm amplifier.

1. Introduction

Current operational amplifiers (COAs) are the key elements in a wide range of analog/digital/mixed signal processing, biomedical and aerospace applications [1-2].

Nomenclatures

A_i	Current gain
f_T	Unity gain frequency
g_m	Transconductance
R _m	Transresistance
r_o	Transistors' output impedance
r_π	Transistors' input impedance

Greek Symbols

α	The ratio of maximum output current to bias current of output transistors
β	BJT transistors' current gain parameter
λ	Current mirrors' gain factor

Abbreviations

AZKA	Azhari Kabi cell
BJT	Bipolar junction transistors.
COA	Current operational amplifier.
CFOA	Current feedback operational amplifier.
CMRR	Common mode rejection ratio.
CMFK	Common mode feedback.
FD	Fully differential.
FVF	Flipped Voltage Follower.
FOM	Figure of merit.
OTA	Operational transconductance amplifier.
P _d	Power dissipation.
PSRR	Power supply rejection ratio.
SOC	System on chip.
THD	Total harmonic distortion.
VOA	Voltage operational amplifier.

They are also key building blocks of current mode signal processing which in recent years has attracted considerable attention due to its superior characteristics such as high speed, low voltage operation, wide dynamic range, etc. [3-4]. However such distinguished capabilities of current mode signal processing can be better achieved by using a fully current-mode signal processing whose arrangement has become possible since AZKA cell being introduced [5]. Otherwise any voltage mode circuit with its internal high impedance nodes in the arrangement of current mode signal processing will deteriorate the high performance of the current mode signal processing. To realize such an arrangement, COA seems an ideal block which based upon the application, may be used either alone or proceeded with a suitable configuration of AZKA Cell [5]. Another important issue is that a COA can be such arranged to perform all functions of a voltage-mode operational amplifier (VOA) while preserving the advantages of current-mode processing [6-8]. So many salient features evident the vital role of COA in analog signal processing.

COAs are found in two main structures: 1) single input differential output structure shown in Fig. 1(a) which is the adjoint block of the conventional differential input single output VOA and 2) Fully differential structure (differential input differential output) shown in Fig. 1(b) which is the adjoint block of the conventional differential input differential output VOA[9].

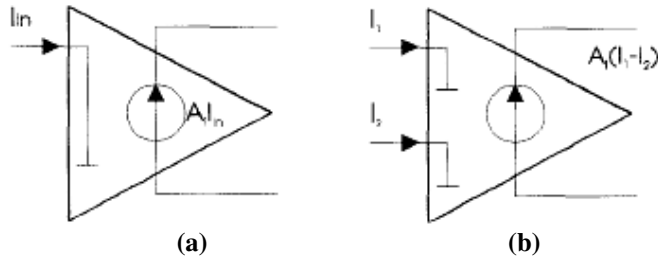


Fig. 1. Circuit Symbol of COA and Its Voltage Mode Counterpart.
 a) Single Input Differential Output, b) Fully Differential [9].

A fully differential COA is preferred to single input differential output COA firstly because fully differential signal processing has inherent immunity to common mode signals, clock feed through, interferences and other types of common mode disturbances [10-11], and secondly a fully differential COA has more flexibility and can be employed as a single input differential output COA if needed.

Block diagram of a fully differential COA is shown in Fig. 2. It usually consists of three main blocks: input stage, gain stage and output stage. Input stage of COA should have low input impedance, gain stage provides high current gain and finally output stage should have high output impedance [1]. The whole structure should also have high current drive capability with low bias current in order to preserve low power consumption. Low input impedance (ideally zero) and a very high (ideally infinite) output impedance of COA makes its design far more different from traditional voltage mode operational amplifiers.

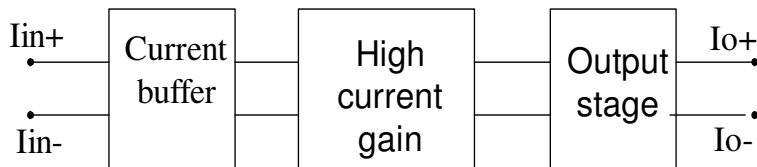


Fig. 2. Block Diagram of Fully Differential COA.

While the high input impedance characteristic of MOS transistors makes them very useful in designing voltage mode operational amplifiers, but maintaining low input impedance and high current gain required for COA is very difficult in CMOS technology. This is due to the fact that the g_m (transconductance) of MOS transistors is low and direct amplification of current signals is not possible using MOS transistors. Thus in CMOS technology COA is mostly realized in such arrangements that contain cascaded transresistance-

transconductance (Rm-Gm) structure [9, 12-19]. This arrangement suffers from the limited bandwidth which is clearly against the one of the most significant advantages of the Current-Mode approach (i.e. High speed/frequency operation). In fact Rm-Gm structure contains at least one high impedance node (usually the output node of Rm amplifier) which limits the bandwidth of COA. On the other hand, current gain of this topology is determined by the product of Rm.Gm that is to obtain high current gain, a high impedance node should be created in the circuit resulted in lower bandwidths.

Thus to implement current mode circuits, BJT transistors are preferred to MOS ones and recently several high performance current mode circuits are implemented in BIPOLAR technology [20-27]. This is due to the fact that BJT transistors have such outstanding properties as; directly amplifying of current signals (with a current gain of β) and larger Gm which results lower input impedance. Bipolar transistors have also much wider current range, wider dynamic range, lower noise, and larger f_T [28]. Whatsoever less approaches (only fully differential COA of [6] and single input differential output COA of [20]) are seen in designing of BJT based COAs which is mainly due to the popularity and dominance of CMOS technology. Besides, existing BJT based COAs have neither shown the expected performance.

In the current work, using BJT transistors a novel fully differential COA is introduced which takes full advantage of current-mode signal processing and shows superior performance over other reported fully differential COAs. Combining some novel ideas allows the proposed COA to provide low input impedance, high f_T , high current gain potential, and high output current to bias current ratio, very small input offset voltage while providing a high common mode rejection ratio (CMRR) too. Its performance is compared with other reported fully differential COAs and some applications based on it are introduced.

The arrangement of this paper is as follows: in section 2 structure of the proposed COA is presented, simulation results are presented in section 3, section 4 includes some applications of the proposed COA and finally section 5 concludes the paper.

2. Proposed Current Operational Amplifier

The complete structure of the proposed COA is shown in Fig. 3(a). It consists of a low input impedance current buffer as input stage implemented by transistors Q_0 - Q_8 and Q'_0 - Q'_8 along with current sources I_{B1} . The gain stage is constructed by Q_9 - Q_{18} transistors and current source I_{B2} - I_{B3} . Due to the fully differential structure of the proposed COA common mode control is required [29] which is done by common mode feedback circuit composed of Q_{C1} - Q_{C6} and I_{B2} current source as is shown in Fig. 3(b). High output impedance cascode current mirrors formed with transistors Q_{19} - Q_{28} is used as output stage. The simple miller compensation approach with nulling resistors is applied to the proposed COA in order to provide proper phase margin. Resistors R_{C1} - R_{C2} and capacitors C_{C1} - C_{C2} are connected between the input and outputs of second gain stage for frequency compensation. The three stages of the proposed COA are detailed as follows:

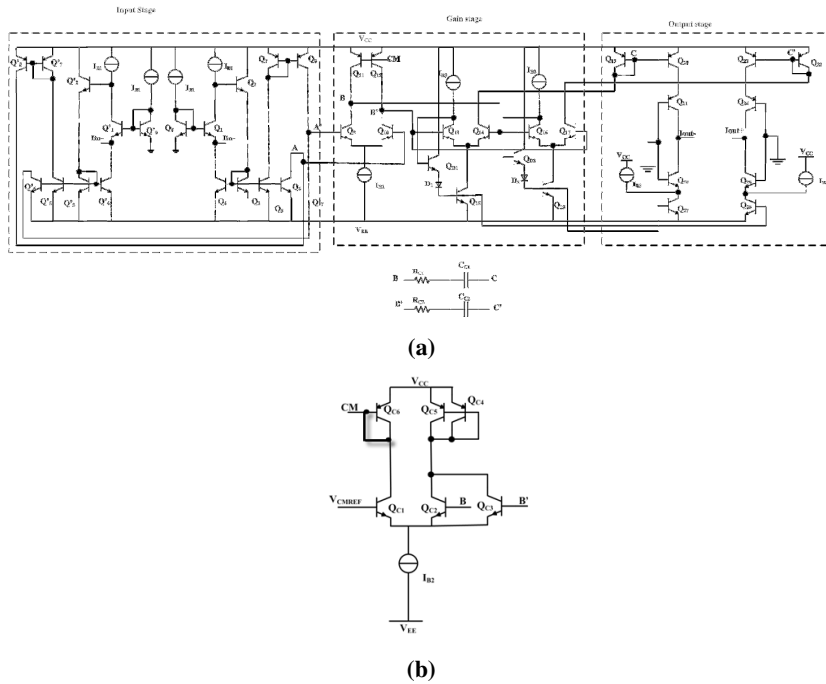


Fig. 3. The complete Structure of a) The Proposed Fully Differential COA, b) The Used Common Mode Feedback.

2.1. Analysis of the input stage

Literature survey shows that to date low input impedance in current mode circuits is achieved employing positive or negative feedback approaches. In some current mode circuits positive feedback is used to reduce input impedance. For example input impedance of 8.2 Ω and 109 Ω are reported in [11] and [16] respectively employing positive feedback technique. However achieving very low input impedances is not practical with positive feedback schemes. This is mainly due to the fact that in positive feedback schemes, a safe margin has to be kept to avoid instability and negative input impedances.

Negative feedback is another method to achieve low input impedance in current mode circuits which has been widely used. It does not have the negative input impedance problem of positive feedback approach. Negative feedback approach also provides wider frequency performance compared to positive feedback one. Hence in order to avoid negative input impedance and provide high frequency performance for the COA, negative feedback approach is employed in the design of input stage.

Input stage consists of input transistors Q1 and Q1'. Negative feedback is performed by Q2-Q4 and Q2'-Q4' transistors and current source IB1 which is used to provide bias current for current buffer transistors. It can be proved that input resistance is given by:

$$R_{in} \approx \frac{1/g_{m1}}{1 + \beta} \tag{1}$$

In Eq. (1) g_{m1} denotes the small signal transconductances of Q_1 and Q'_1 transistors respectively defined as IC/V_T where V_T is the thermal voltage approximately equal to 26 mV at room temperature and β is the current gain of Q_2 and Q'_2 transistors.

Diode connected transistors Q_0 and Q'_0 , keep the input node voltage at ground potential resulting in an approximately zero offset voltage at the input node. NPN current mirrors formed with Q_5 - Q_6 , Q'_5 - Q'_6 along with PNP current mirrors formed with Q_7 - Q_8 and Q'_7 - Q'_8 provide differential outputs for the input stage. The elaborately connection of PNP and NPN current mirrors, results in an effective cancellation of common mode currents at the output of input stage and increase of the overall CMRR of the proposed COA.

2.2. High current gain stage

The gain stage is composed of two cascaded amplifier stages; a conventional differential amplifier implemented with transistors Q_9 - Q_{12} (accompanied with a common mode feedback block consists of Q_{C1} - Q_{C6} and tail current source I_{B2}); followed by a novel class AB gain stage formed by Q_{13} - Q_{18} transistors and current sources I_{B3} . The common-mode feedback block [30] stabilizes the common mode level of nodes B and B' to V_{CMREF} .

The differential input currents transferred to nodes A and A' are then injected to the base of Q_9 and Q_{10} due to high output impedance of Q_7 - Q_8 and Q'_7 - Q'_8 compared to differential mode input impedance of differential pair and amplified by factor of β_9 and β_{10} resulting in a differential mode current gain of:

$$\frac{I_{O9}}{I_{ind}} = \frac{r_{o8} \parallel r_{o7}'}{r_{o8} \parallel r_{o7}' + r_{\pi9}} \times \beta_9 = \frac{I_{O10}}{I_{ind}} = \frac{r_{o8} \parallel r_{o7}}{r_{o8} \parallel r_{o7} + r_{\pi10}} \times \beta_{10} \quad (2)$$

where r_o , r_{π} and β are the i^{th} transistor output impedance, input impedance and current gain respectively.

The output currents of Q_9 and Q_{10} are amplified by the second gain stage. Current amplification in the second gain stage is done by Q_{14} and Q_{17} transistors which (instead of constant current sources) are biased with flipped voltage followers[31] (FVF) composed of Q_{13} , Q_{15} , Q_{D1} and Q_{16} , Q_{18} , Q_{D2} transistors, diodes D_1 - D_2 and current source I_{B3} . CMOS version of FVF is widely used in the design of OTA [32]. In this paper for the first time, BJT version of FVF is used in the gain stage in a novel way. In the BJT version of FVF, Diodes D_1 and D_2 are inserted at the base node of Q_{15} and Q_{18} for level shifting purpose and Q_{D1} , Q_{D2} are used for both level shifting and reducing the effect of the base current of Q_{15} and Q_{18} on I_{B3} and providing a constant current equal to I_{B3} for Q_{13} and Q_{16} .

Actually, the base current of Q_{18} and Q_{15} are attenuated by Q_{D1} and Q_{D2} by a factor of β_{QD1} and β_{QD2} which reduces their effect on I_{C13} and I_{C16} respectively providing an approximately fixed current of I_{B3} for them. Due to the symmetry, the bias current of Q_{14} and Q_{17} will also be set to I_{B3} . Owing to the elaborately arrange of components, in the second gain stage, the bias current of Q_{14} and Q_{17} are equal to I_{B3} while they can sink large amount of current from V_{DD} through Q_{15} and Q_{18} respectively.

The operation of the proposed class AB gain stage can be explained as follows: The output current from the first gain stage at node B; due to the fixed current of

Q_{16} ; enters to the base of Q_{14} and amplified by a current gain of β_{14} . Similarly output current at node B' enters to the base node of Q_{17} and amplified by gain of β_{17} . It is worth nothing that the amplified current by Q_{14} and Q_{17} can be much larger than their bias currents which stems from large current drive capability of FVF. Thanks to the FVF blocks which provides proper bias current for the second gain stage as well as high current drive capability. It can be shown that the differential mode current gain at the collectors of Q_{14} and Q_{17} can be found as:

$$\frac{I_{CQ14}}{I_{ind}} = \frac{I_{CQ17}}{I_{ind}} \approx \beta_9 \times \beta_{14} \times \frac{r_{o8} \parallel r_{o7}'}{r_{o8} \parallel r_{o7}' + r_{\pi9}} = \beta_{10} \times \beta_{17} \times \frac{r_{o8} \parallel r_{o7}}{r_{o8} \parallel r_{o7} + r_{\pi10}} \quad (3)$$

2.3. The output stage

The identification of the location of the centre of pressure of a projectile body is motivated by the need for calculating aerodynamic moments, stability and structural analyses. The centre-of-pressure location of bodies composed of conical noses and cylindrical afterbodies is determined as follows [7]:

The output stage is required to mainly have high output impedance and high current drive capability. The overall CMRR of the COA can also be further increased by such designing the output stage that cancels the common mode currents. Such requirements are carefully considered in the design of the output stage of the proposed COA. By considering the fact that collector current of Q_{14} and Q_{17} are approximately equal to the collector current of Q_{15} and Q_{18} respectively, the operation of the proposed output stage can be explained as follows:

The amplified current of IC_{14} is transferred to the negative output node by Q_{19} - Q_{20} PNP current mirror at the upper branch. IC_{18} (which is equal to IC_{17}) is also transferred to the negative output node by Q_{27} NPN transistor at the lower branch. The connection of PNP current mirror of Q_{19} - Q_{20} and NPN transistor Q_{27} aims to cancel the common mode signals of Q_{14} and Q_{17} at the output node by subtracting them from each other meanwhile introducing an intrinsic amplification of two for differential mode ones. This elaborately composed structure grants the overall COA very high CMRR. Similarly IC_{17} is transferred to the positive output node i.e out- through Q_{22} - Q_{23} PNP current mirror at the upper branch where are subtracted from IC_{15} which is transferred to the output node by Q_{26} NPN transistor at the lower branch. In the output stage well combination of the PNP cascode current mirrors and NPN transistors provides very high output impedance while preserving high CMRR. The simple structure of the proposed output stage also yields low power consumption and high frequency performance. The current of PNP current mirrors of Q_{19} - Q_{20} , Q_{22} - Q_{23} and NPN transistors Q_{26} , Q_{27} at the output stage are directly provided by the previous class AB gain stage. Thus the output stage has also class AB configuration which makes the overall COA capable of handling higher currents compared to the bias current.

It is worth noting that the bias current of Q_{26} and Q_{27} are equal to $2IB_3$ while the bias current of PNP current mirrors is equal to IB_3 . This will introduce an offset current equal to IB_3 at the output nodes. Such an undesired offset current can be simply cancelled by connecting two current sources equal to IB_3 at the collectors of Q_{26} and Q_{27} as is shown in Fig. 3.

2.4. The small signal parameters of the proposed COA

From the previous sections we conclude the small signal parameters of the proposed COA as:

$$R_{in} \approx \frac{1/g_{m1}}{1 + \beta_{Q2}} \quad (1)$$

$$Ai \approx 4 \times \beta_9 \times \beta_{14} \times K = 4 \times \beta_{10} \times \beta_{17} \times K \quad (4)$$

$$CMRR \approx (1 + 2 \cdot gm_9 \cdot R_{EE2}) \times \left(\frac{2}{1 - \alpha} \right) \times \frac{1}{(\lambda_1 - \lambda_2)} \times \frac{1}{(\lambda_3 - \lambda_4)} \times A_{CMFK} \quad (5)$$

$$R_{out} = \beta_{21} r_{o21} \parallel r_{o28} r_{o27} \quad (6)$$

$$K = \frac{r_{o8} \parallel r_{o7}}{r_{o8} \parallel r_{o7} + r_{\pi9}} = \frac{r_{o8} \parallel r_{o7}}{r_{o8} \parallel r_{o7} + r_{\pi10}} \quad (7)$$

$$\lambda_1 = \frac{\beta_{Q7}}{2 + \beta_{Q7}} = \frac{\beta_{Q7}}{2 + \beta_{Q7}} \quad (8)$$

$$\lambda_2 = \frac{\beta_{Q4}}{4 + \beta_{Q4}} = \frac{\beta_{Q4}}{1 + \beta_{Q4}} \quad (9)$$

$$\lambda_3 = \frac{\beta_{Q19}}{2 + \beta_{Q19}} = \frac{\beta_{Q22}}{2 + \beta_{Q22}} \quad (10)$$

$$\lambda_4 = \frac{\beta_{Q15}}{1 + \beta_{Q15}} = \frac{\beta_{Q18}}{1 + \beta_{Q18}} \quad (11)$$

$$A_{CMFK} = \frac{gm_{QC1}}{gm_{QC6}} \quad (12)$$

where α is the voltage gain of VVF, λ_1 and λ_2 are current gains of PNP and NPN current mirrors at the input stage respectively, λ_3 and λ_4 are current gains of upper and lower cascode current mirrors at the output stage respectively, R_{EE2} is the output impedance of current source IB_2 , β_i and r_{oi} are the current gain and output impedance of the related transistor respectively, and A_{CMFK} is the gain of common mode feedback circuit.

3. Simulation Results

Simulations of the proposed COA of Fig. 3 are performed using 0.8 μm -BICMOS technology bipolar transistors parameters with PSPICE. The values of used elements and bias sources are summarized in Table 1. Real current sources were implemented through simple current mirrors.

Figure 4 shows the current gain (Ai) bode plot of the proposed COA which shows 82.4 dB DC gain and 52.3° phase margin. Its -3 dB bandwidth and unity gain frequency are 486.3 kHz and 698 MHz respectively.

Figure 5 shows the response of the proposed COA to step input of $\pm 100 \mu\text{A}$ in unity gain configuration which proves its closed loop stability. The CMRR Frequency performance of the proposed COA is shown in Fig. 6 which shows a CMRR of 179 dB with high f_T of 2.6 GHz. Moreover the proposed COA has high PSRR. The simulated positive and negative PSRR are 182 dB and 196 dB respectively which mainly stems from the fully differential configuration of the

proposed COA. Favourably the used negative feedback at the input stage has resulted in a low input impedance of 31 Ω and output impedance of 31.7 MΩ.

Due to the use of FVF based gain stage, the proposed COA can deliver up to ±1.5 mA output current (the large ratio of 25 for output current compared to 60μA bias current of output transistors) at a THD of -40 dB. Figure 7 shows the input-output Trans characteristic in unity-gain configuration, which also clearly proves the high current drive capability of the proposed COA.

The simulation results show that the proposed COA consumes a total power of 2 mW from a ±1.2 V supply, while its input offset voltage is about -0.7 mV. The amplifier characteristics are summarized in Table 2.

To have a fair comparison between reported COAs in [6, 11-18] which are gathered in Table 3, first a figure of merit is defined as in Eq. (13). It includes eight important performance parameters of COA namely; output resistance (R_{out}), current gain (A_i), common mode rejection ratio ($CMRR$), unity gain frequency(f_T), input resistance (R_{in}), power dissipation (P_d), the ratio of maximum output current to the bias current of output transistors(α) and supply voltage (V_{DD}) according to Eq. (13)

$$FOM = \frac{R_{out} \times A_i \times CMRR \times f_T \times \alpha}{V_{DD} \times R_m \times P_d} \quad (13)$$

Last column of Table 3 include the calculated FOM for the reported COAs. To calculate the defined FOM, parameters that are not reported in the related works (marked as NA) are omitted from Eq. (13). As can be seen, the proposed COA has the largest FOM compared to others.

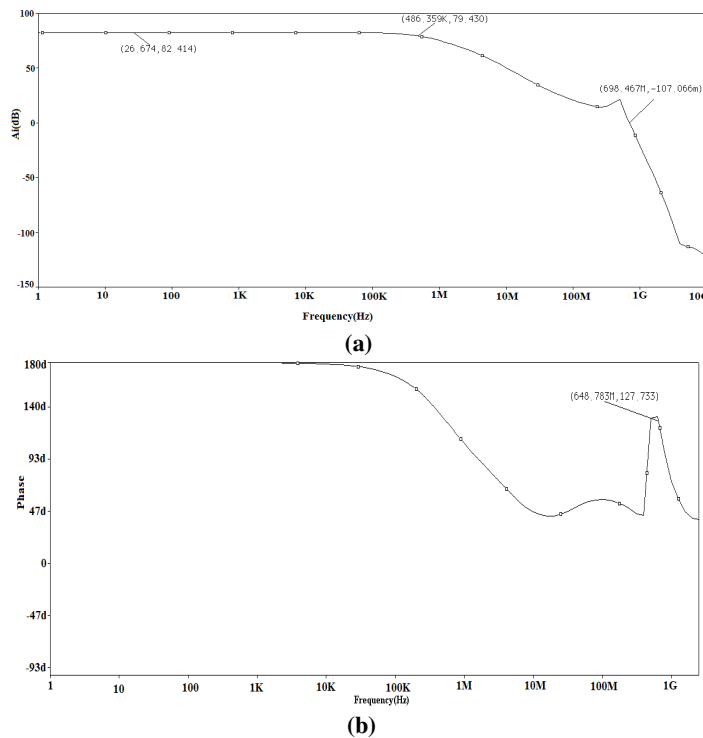


Fig. 4. Frequency Performance of the Gain; a) Magnitude, b) Phase.

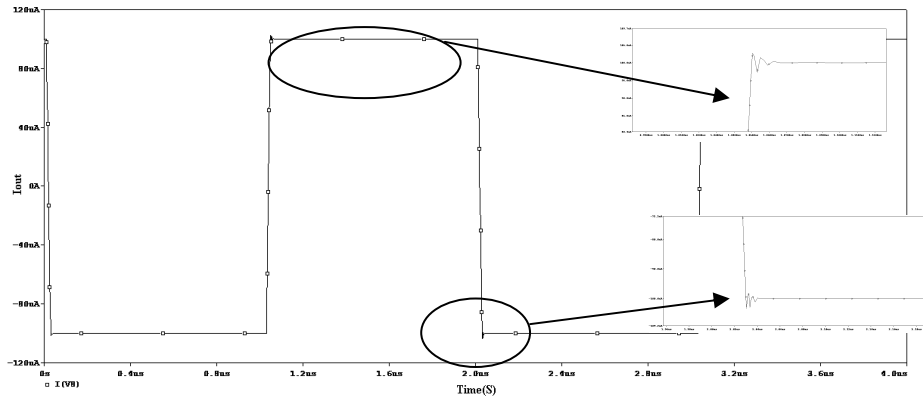


Fig. 5. Step Response of the Proposed COA in Unity Gain Configuration.

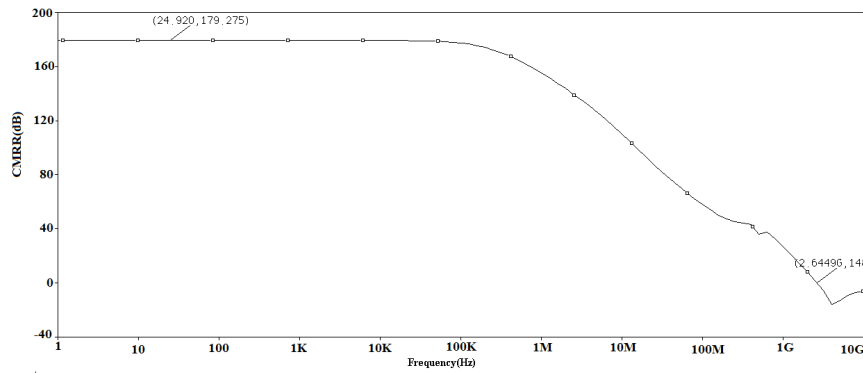


Fig. 6. Frequency Performance of CMRR.

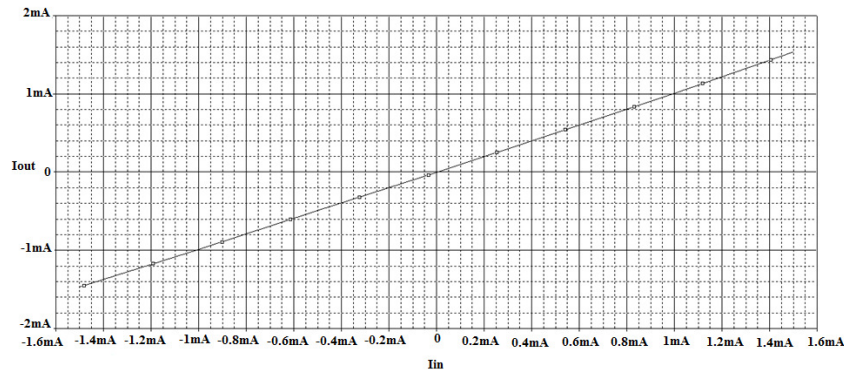


Fig. 7. Input Output Trans Characteristic of the Proposed COA in Unity Gain Configuration.

Table 1. Used Bias Currents and Voltages and Passive Elements' Values.

Element	I_{B1}	I_{B2}	I_{B3}	$V_{CC}-V_{EE}$	$R_{C1}-R_{C2}$	$C_{C1}-C_{C2}$	V_{CMREF}
Value	10 μ A	100 μ A	60 μ A	\pm 1.2 V	1 k Ω	4 pF	0.5 V

Table 2. Summary of the Proposed COA Simulation Results.

Parameter	Value
DC	82.4 dB
A_{id} f-3 db	486.3 kHz
f_T	698 MHz
Phase margine after compensation	52.3°
R_{in}	31 Ω
R_{out}	31.7 M
CMRR	179 dB
PSRR (+/-)	182 dB/196 dB
Input offset voltage	-0.7 mV
Maximum output current($I_{out_{max}}$)	± 1.5 mA
Drive capability ($I_{out_{max}}/I_B$)	25
Power dissipation	2 mW

Table 3. Comparison between Reported Fully Differential COAs and the Proposed One.

Ref/Pub. Year	R_i (Ω)	R_o (M Ω)	A_i (dB)	f_T (MHz)	CMRR (dB)	VDD (V)	P_d (mW)	α	FOM (dB)
[6]B/1986	210	0.087	86	NA	106	± 15	NA	NA	214
[7]B/1980	NA	5.4	NA	NA	NA	15	NA	NA	111.12
[9]C/1997	NA	NA	57.71	314	41.25	± 1.5	6.5	1	297
[12]C/1994	316	0.316	67	100	150	3	4.5	NA	474
[13]C/1993	NA	NA	72	3	NA	NA	NA	NA	201.54
[14]C/1997	NA	NA	75-96	145	NA	± 15	<0.5	NA	295 ⁽¹⁾
[15]C/2005	23.16	15.38	65.5	266	89.5	± 1.5	4.07	1	478.2
[16]C/2008	124 109 ⁽²⁾	30	96	92	NA	± 1.5	0.66	1	418.13*
[17]C/1998	21	0.597	53	300	52	3	< 0.86	NA	415
[18]C/2007	1.6K	6100	100	85	NA	± 1.5	0.72	17.5	456
[19]C/1999	NA	NA	90	11	NA	5	NA	NA	216.84
Pro. ⁽³⁾	31	31.7	82.4	698	179	± 1.2	2	25	632

(1) Maximum FOM, (2) different positive (124) and negative (109) input resistances, (3) Proposed, B: Bipolar Technology, C: CMOS Technology

4. Some Applications of the Proposed COA

In this section, the proposed COA is used to realize a voltage amplifier and an Rm amplifier as follows

4.1. Realization of a high bandwidth voltage amplifier with COA

COA can be used to realize high performance voltage amplifier as is shown in Fig. 8 [8]. Because COA has better frequency performance compared to VOA, this voltage amplifier can operate at higher frequencies compared to the one constructed by traditional VOA. On the other hand the configured voltage amplifier has gains independent from their -3 dB bandwidth. In the voltage amplifier of Fig. 8 the input node is at ground potential, hence the input voltage is converted into currents through resistor R1 which is then converted back to voltage through resistor RF. In Fig. 7 the voltage gain is given by (14):

$$A_v = \frac{V_{out}}{V_i} \approx -\frac{R_F}{R_1 + R_{in}} \times \frac{A_i}{1 + A_i} \approx -\frac{R_F}{R_1} \times \frac{A_i}{1 + A_i} \quad (14)$$

By assuming single pole frequency performance for COA as:

$$A_i = \frac{A_0}{1 + \frac{S}{P_0}} \quad (15)$$

(where A_0 and P_0 are the DC gain and -3 dB frequency of COA respectively) and manipulating Eq. (14), we get:

$$A_v = -\frac{R_F}{R_1} \times \frac{A_0}{1 + A_0} \times \frac{1}{1 + \frac{S}{A_0 \cdot P_0}} = -\frac{R_F}{R_1} \times \frac{A_0}{1 + A_0} \times \frac{1}{1 + S/f_T} \quad (16)$$

and f_T is the unity gain frequency of COA.

As can be seen from Eq. (16), all closed loop voltage gains will have the same -3 dB bandwidth equal to unity gain frequency of COA. Although this property has been found in CFOA, but it is there achieved at the expense of reduced accuracy [33].

Figure 9 shows the simulation results of the voltage amplifier of Fig. 8 in which R_F is constant and R_1 is a varied parameter. The results demonstrate a gain independent bandwidth of approximately 546 MHz which is very close to unity gain frequency of COA.

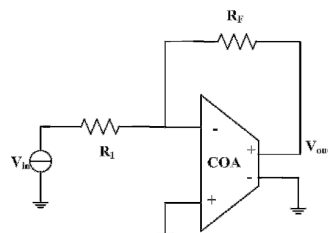


Fig. 8. The Proposed COA Voltage Gain Configuration.

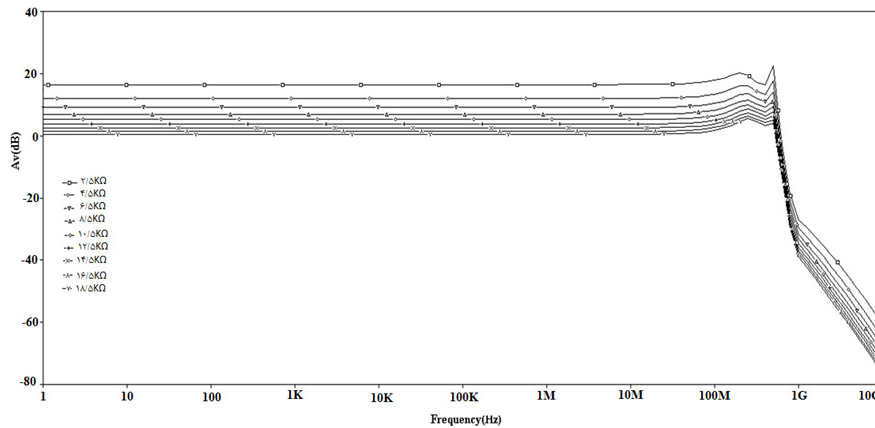


Fig. 9. The Configured VOA Frequency Response for $R_F=20 \text{ k}\Omega$ and R_1 Varied Linearly from $1 \text{ k}\Omega$ to $20 \text{ k}\Omega$ in $2 \text{ k}\Omega$ steps.

4.2. Application of the proposed COA as an Rm amplifier

The application of proposed COA to realize a high performance Rm amplifier is shown in Fig. 10 [6]. The parameters of Rm amplifier are found as [6]:

$$A = Rm = \frac{V_o}{I_{in}} = \frac{-R \times A_i}{1 + A_i} \tag{17}$$

$$Z_{in} = \frac{R_{in}}{A_i} \tag{18}$$

$$Z_o = \frac{R}{A_i} \tag{19}$$

where R_{in} is the input impedance of COA. By inserting Eq. (15) into Eqs. (17)-(19) we get:

$$A = Rm = \frac{V_o}{I_{in}} \approx \frac{-R \times A_0}{1 + \frac{S}{f_T}} \tag{20}$$

$$Z_{in} = \frac{R_m}{A_i} = \frac{R_{in}}{A_0} \times \left(1 + \frac{S}{P_0}\right) \tag{21}$$

$$Z_o = \frac{R}{A_i} = \frac{R}{A_0} \times \left(1 + \frac{S}{P_0}\right) \tag{22}$$

The frequency performance of Rm amplifier is shown in Fig. 11 for $R=3\text{ k}\Omega$ which shows -3 dB bandwidth of 649 MHz. The frequency performance of input and output impedances of the Rm amplifier are shown in Figs. 12 and 13 respectively. The achieved values are 2.4 m Ω and 0.419 Ω for the input and output impedances respectively which are in good agreement with Eqs. (20)-(22).

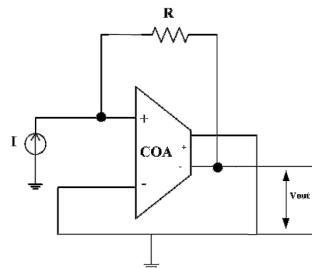


Fig. 10. Application of COA as an Rm Amplifier [6].

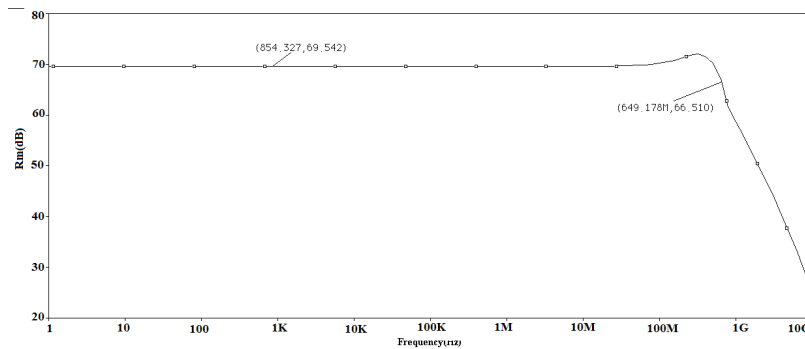


Fig. 11. Frequency Performance of Rm Amplifier for $R=3\text{ k}\Omega$.

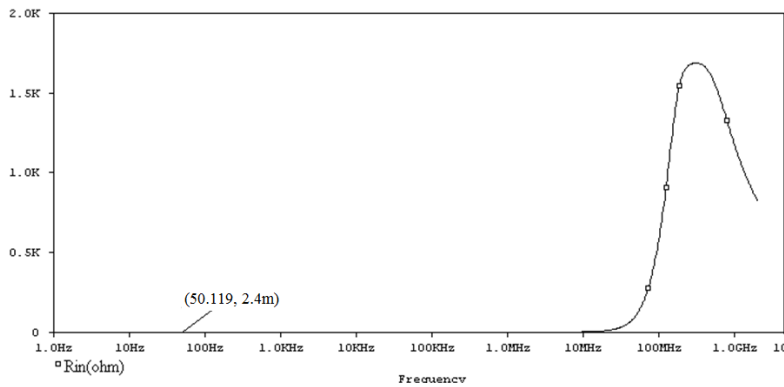


Fig. 12. Frequency Performance of the Input Impedance of the COA Based Rm amplifier for $R=3$ k Ω .

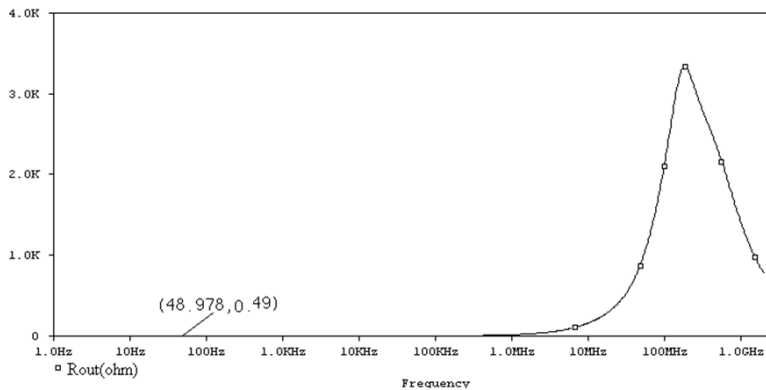


Fig. 13. Frequency Performance of the Output Impedance of the COA Based Rm Amplifier for $R=3$ k Ω .

5. Conclusions

A new BJT based fully-differential COA is presented. Employing several innovative ideas provided the designed COA with excellent performance especially in frequency performance, input resistance, CMRR, output current drive capability and output resistance. Based on the use of a FVF based current gain cell, high current drive capability is achieved.

The theoretical analysis of the COA operation is presented. The COA is implemented using 0.8 μm BICMOS technology and simulated by PSPICE. Comparing the results with the parameters of some of the existing premium COAs implies that the present design by its own takes the lead of the whole group especially in terms of CMRR and f_T .

The use of the proposed COA to realize a constant bandwidth voltage amplifier and a high performance Rm amplifier have been demonstrated. These results give strong motivation for the development of an integrated current amplifier which can be used where the traditional VOA fails to operate desirably.

References

1. Palmisano, G.; Palumbo, G.; and Pennisi, S. (1999). *CMOS current amplifiers*. Kluwer Academic Publishers.
2. Wang, Z. (1990). Wideband class AB(push-pull) current amplifier in CMOS technology. *Electronics Letters*, 26(8), 543-545.
3. Toumazou, C.; Lidgey, F.; and Haigh D. (1990). *Analogue IC design: The Current-Mode approach*. IEE.
4. Rajput, S.S.; and Jamuar, S.S. (2002). Low voltage analog circuits design technique. *IEEE Circuit and System Magazin*, 2(1), 24-42.
5. Azhari, S.J.; and Kaabi, H. (2000). AZKA cell, the current mode alternative of Wheatstone bridge. *IEEE Transactions on Circuits and Systems-I: Fundamental Theory and Applications*, 47(9), 1277-1284.
6. Toumazou, C. (1986). *The universal current amplifiers*. Ph.D Thesis, Imperial Colledge London
7. Allen, P.E.; and Terry, M.B. (1980). The use of current amplifier for high performance voltage applications. *IEEE Journal of Solid State Circuits and Systems*, 15(2), 155-162.
8. Pyne, A.; and Toumazou, C. (1996). Analog amplifiers: Classification and generalisation. *IEEE Transaction on Circuits and Systems-I: Fundamental Theory and Application*, 43(1), 43-50.
9. Cheng, K.; and Wang, H. (1997). Design of current mode operational amplifier with differential-input and differential-output. *Proceedings of the IEEE International Symposium on Circuits and Systems*, 1, 153-156.
10. Mahmoud, S.A. (2006). New fully differential CMOS second generation current conveyor. *ETRI Journal*, 28(4), 495-501.
11. Azhari, S.J.; and Safari, L. (2010). A high CMRR low power fully differential current buffer. *IEICE Electronics Express*, 7(11), 765-771.
12. Abou-Allam, E. and El-Masry, E.I. (1994). High CMRR CMOS current operational amplifier. *Electronics Letters*, 30(73), 1042-1043.
13. Kaulberg, T. (1993). A CMOS current-mode operational amplifier. *IEEE Journal of Solid-State Circuits*, 28(7), 849-852.
14. Assi, A.; Sawan, M.; and Raut, R. (1997). A fully differential and tunable CMOS current mode opamp based on transimpedance-transconductance technique. *Proceedings of the 40th Midwest Symposium on circuits and Systems*, 1, 168-171.
15. Youssef, M.A.; and Soliman A.M. (2005). A novel CMOS realization of the differential input balanced output current operational amplifier and its applications. *Analog Integrated Circuits and Signal Processing*, 44(1), 37-53.
16. Altun, M.; and Kuntman, H. (2008). Design of a fully differential current mode operational amplifier with improved input-output impedances and its filter applications. *AEU: International Journal of Electronics and Communications*, 62(3), 239-244.
17. Jun, S.; and Kim, D.M. (1998). Fully differential current operational amplifier. *Electronics Letters*, 34(1), 62-63.
18. Altun, M.; and Kuntman, H. (2007). A high drive fully differential current mode operational amplifier providing high output impedance and filter

- application. *Proceedings of the 5th International Conference on Electrical and Electronics Engineering, Electronics, Bursa, Turkey*, 44-47.
19. Palmisano, G.; and Penissi, S. (1999). A versatile fully differential current amplifier. *Proceedings of the 6th IEEE International Conference on Electronics, Circuits and Systems*, 2, 607-610.
 20. Nagasaku, T.; Hyogo, A.; and Sekine, K. (1996). Synthesis of a novel current operational amplifier. *Analog Integrated Circuits and Signal Processing*, 11(2), 183-185.
 21. Kubota, K. and Okine, M. (2002). Realization of a multiport gyrator using current mirror circuit. *Electrical Engineering in Japan*, 139(4), 41-47.
 22. Kashtiban, M.H.; and Azhari, S.J. (2009). A novel wideband-high-CMRR low-voltage BJT current output stage. *Proceedings of European Conference on Circuits Theory and Design*, 691-694.
 23. Yuce, E. (2009). Current-mode electronically tunable biquadratic filters consisting of only CCCIs and grounded capacitors. *Microelectronics Journal*, 40(12), 1719-1725.
 24. Somdunyanok, M.; Pattanathadapong, T.; and Prommee, P. (2008). Accurate tunable current-mirror and its applications. *International Symposium on Communications and Information Technologies*, 56-61.
 25. Yang, B.-D.; Kim, J.-S.; Yun, J.-K.; Lee, Y.-K.; and Lee J.-S. (2008). A highly accurate BiCMOS cascode current mirror for wide output voltage range. *IEEE International Symposium on Circuits and Systems*, 2314-2317.
 26. Sawangarom, V.; Tangsrirat, W.; and Surakampontom, W. (2006). NPN-based current differencing buffered amplifier and its application. *International Joint Conference SICE-ICASE, Busan*, 5766-5769.
 27. Arslanalp, R.; and Yuce, E. (2009). A BJT technology-based current-mode tunable all-pass filter. *Microelectronics Journal*, 40(6), 921-927
 28. Kenneth, R.; Willy, L.; and Sansen, M.C. (1994). *Design of analog integrated circuits and systems*. McGraw-Hill Book Company.
 29. Gray, P.R.; Hurst, P.J.; Lewis, S.H.; and Meyer, R.G. (2001). *Analysis and design of analog integrated circuits*. (4th Ed.) Wiley.
 30. Hwang, J.-H.; and Yo, C. (2004). A low-power wide-bandwidth fully differential operational amplifier with current re-using feedforward frequency compensation. *IEEE Asia-Pacific Conference on Advanced System Integrated Circuits*, 32-35.
 31. Carvajal, R.G.; Ramirez-Angulo, J.; Lopez-Martin, A.J.; Torralba, A.; Galan, J.A.G.; Carlosena, A.; and Chaverro, F.M. (2005). The flipped voltage follower: A useful cell for low voltage low power circuit design. *IEEE Transactions on Circuits and Systems-I: Regular Papers*, 52(7), 1276-1291.
 32. Lopez-Martin, A.J.; Baswa, S.; Ramirez-Angulo, J.; and Carvajal, R.G. (2005). Low-voltage super class AB CMOS OTA cells with very high slew rate and power efficiency. *IEEE Journal of Solid State Circuits*, 40(5), 1068-1077.
 33. Palumbo, G.; and Pennisi, S. (2001). Current-feedback versus voltage operational amplifiers. *IEEE Transactions on Circuits and Systems-I: Fundamental Theory and Applications*, 48(5), 617-623.